UNIVERSITY OF BIRMINGHAM

University of Birmingham
Research at Birmingham

Comparing the viscoelastic properties of gelatin and different concentrations of kappa-carrageenan mixtures for additive manufacturing applications

Warner, E.l.; Norton, I.t.; Mills, T.b.

Link to publication on Research at Birmingham portal

Comparing the viscoelastic properties of gelatin and different concentrations of kappa-carrageenan mixtures for additive manufacturing applications

E. L. Warner*, I. T. Norton and T. B. Mills

School of Chemical Engineering, University of Birmingham, Edgbaston, B15 2TT, UK

*Corresponding author. E-mail address: ELW198@bham.ac.uk

Abstract

Recent interest in personalisation of food through additive manufacturing has identified a need for more information on the formulation and printability of potential ingredients. The printability of four different mixtures of two food hydrocolloids, gelatin and kappa-carrageenan were investigated. Design rules were established to determine whether the materials fit the requirements of the process. The gelling temperatures of the systems and the rheological characteristics including: flow profiles, evolution of elastically dominated structures and frequency dependent behavior were established. The mixtures were subsequently printed at two temperatures, just above and much greater than, the gelling temperatures. Analysis showed the rheological behaviours accompanying the coil-helix transitions of the systems were key to printing the product in a well-defined manner. Printing fidelity was related to the changes in elastic modulus, where rapid formation of an elastic network gave rise to defined shapes with the ability to self-support under multiple layers.

Keywords

Additive manufacturing; gelatin, kappa-carrageenan; microstructure; rheology; printability.

1. Introduction

The use of additive manufacturing to be able to design and control the microstructure within food products has a huge potential for impact on the food industry. It would enable the production of foods with detailed ingredient distribution, resulting in highly efficient use of materials (Diaz et al., 2014). Additionally, additively manufacturing food could also lead to the formulation of products with predefined textural and release properties, tailored to the individual consumer's requirements. Although in theory ideal, the incorporation of this technique into everyday use still has many challenges.

36   One of the most prominent being incorporation of products into the consumer supply

37   chain: requiring the widespread design of printers and formulations capable of printing

38   numerous products. For this reason, much effort is going into understanding the

39   design principles required for printing food products with the aim to translate them into

40   the additive manufacturing field.

41

42   The term "additive manufacturing" encompasses many different techniques, whereby,

43   an object is created through the deposition of materials layer by layer (Godoi et al.,

44   2016). Whilst additive manufacturing techniques such as selective laser sintering

45   (SLS) have been used for the production of food products (Diaz et al., 2016), the main

46   focus of the researched is based on fused deposition modelling (FDM). FDM uses an

47   extrusion/deposition process in order to create 3-dimensional objects. This technique

48   was originally created for use with thermoplastic materials in filament form (Wohlers

49   and Gornet, 2012), worked by motors pulling solid filament into a nozzle where heat

50   is applied to melt the material to create a flowable, fluid state (Crump, 1992). The

51   material is then extruded and deposited onto the build platform, where cooling leads

52   to solidification (Kruth et al., 1998).

53

54   FDM has been slow to move into the food industry, as the complex nature of foods

55   pose many challenges: multi-component, controlled microstructures for sensory

56   attributes, multiple thermal transitions and polymorphs *etc*. For this reason, there is

57   limited literature on the thermal printing of food products, with most of the examples

58   focused around the thermal extrusion of chocolate (Hao et al., 2010). However, a

59   much wider range of materials are required if FDM is going to become a commercially

60   viable option. As such, much of the current research has been focused on the printing

61   of materials through extrusion that are intrinsically thixotropic at room temperature;

62   providing a means of flowing through the nozzle and thickening again without the need

63   of thermal transitions. Cohen et al. (2009) has demonstrated the use of a syringe

64   based FDM process to print combinations of low concentration gelatin and xantham

65   gum. It was shown that it was possible to simulate a wide variety of mouth feels,

66   ranging from systems with sensory attributes for chocolate through to risotto by using

67   these two ingredients. Yang et al. (2018) developed an FDM machine to determine

68   the optimum printing parameters for the printing of lemon juice gel. To ensure that the

69   desired geometry was achieved from the printed shape, Yang and his team

70 investigated different printing parameters, including nozzle height, diameter and
71 movement speed in order to determine their optimum values. These parameters were
72 assessed by printing lines and cylinders while varying the parameters and then visually
73 observing which had printed closest to the target geometry. They determined that a
74 storage modulus (G') of ca. 5 kPa, nozzle height and diameter of 1 mm and a nozzle
75 moving speed of 30 mm/s enabled the printing of the most precise shapes. Although
76 such materials have demonstrated much promise in the field, they are often
77 impractical, being too weak to mechanically manipulate preventing them from being
78 moved/packaged *etc.* One answer to this are thermo-reversible hydrogels, using a
79 thermal process to structure the materials with controlled mechanical properties.
80
81 Gelatin and kappa-carrageenan (κC) are both thermo-reversible polysaccharides
82 commonly used within the food industry. Gelatin is obtained by the partial hydrolysis
83 of collagen, which is derived from animal skin and bones; it is favoured by
84 manufacturers because its body-temperature melting point produces a desirable
85 mouthfeel (Morrison et al., 1999). The gelation of gelatin occurs through the transition
86 of random coils into helices and gels as the temperature is decreased (Joly-Duhamel
87 et al., 2002). κC originates from a family of linear polysaccharides extracted from
88 different species of red algae (Mangione et al., 2005). Gelation of κC has been
89 attributed to the double helix formation which involved regular sequences between the
90 kink point on two adjacent chains (Rees, 1972). Upon the addition of κC to gelatin,
91 there occurred an interaction between the positively charged amine groups within the
92 gelatin and the negatively charged sulfate groups within the κC (Antonov and
93 Gonçalves, 1999). This lead to the formation of (bio)polyelectrolyte complexes, which
94 affected the thermo-stability of the system, increasing the gelation rate (Derkach et al.,
95 2015). The formulation of gelatin alone was a transparent mixture, but upon addition
96 of κC, the mixtures became turbid. This was due to associative phase separation of
97 the two polymers (Antonov and Gonçalves, 1999).
98
99 The properties of the materials to be extruded within the FDM process play a key part
100 in determining whether the material will be printable. Some research has already been
101 undertaken in order to investigate how the rheological properties of different materials
102 affect their printability. Liu et al. (2017) investigated the printability of mashed potato

103   modified with various amounts of potato starch by researching the viscosity and

104   viscoelastic properties. It was established that the ideal addition of potato starch was

105   2%, exhibiting a yield stress of 312.16 Pa and a G' of around 4 kPa. Lower amounts

106   of potato starch produced lower yield stress and the printed objects sagged; the

107   addition of more potato starch led to difficulty in extruding due to the resultant high

108   value of the consistency index (214.27 Pa.s^n). Li et al. (2016) also explored the use

109   of biopolymers, alginate-based hydrogels, in an effort to quantify the quality of 3D

110   prints at ambient temperatures. Here they determined that the thixotropic nature of the

111   gel was key to good printability, a property that could be finely tuned through the

112   addition of graphene oxide, to allow them to manipulate the uniformity of the printed

113   shape.

114

115 Research undertaken to date has concentrated on exploring the rheological properties

116 and printability of hydrogels using materials which maintain their shape due to a yield

117 stress. Whilst this technique is satisfactory, a greater variety of foods and finishes

118 could be provided with the benefit of an enhanced understanding of the material

119 properties necessary in order to print food that transitions from a liquid to a solid.

120

121 The main objectives of this study were, therefore, to investigate the viscoelastic

122 properties of a temperature dependent gelatin-based solution and then correlate these

123 properties with the printability of the material.

124

125   ## 2. Materials and methods

126   ### 2.1. Materials

127 Porcine gelatin (250 bloom), and κC were purchased from Sigma-Aldrich (UK).

128 Reverse osmosis water was used, which had been purified using a millipore purifier.

129 The materials were used without any further purification or modifications.

130

131   ### 2.2. Preparation of the gelatin and κC solutions

132 Four different formulations were investigated, 5% gelatin with 0, 1, 2 and 3% κC. The

133 samples were prepared by dispersing the required amount of κC into the reverse

134 osmosis water at a temperature of 70˚C on a heated bed, under agitation using a

135 magnetic stirrer bar for 30 minutes. Subsequently, the gelatin was added to the

solution, at a temperature of 60˚C, and left to fully hydrate for 30 minutes in correspondence with (Takayanagi et al., 2000), under agitation.

2.3. Characterisation of the formulations

2.3.1. µDSC

A Seteram MicroDSC 3 evo (Seteram, France) was used to analyse the thermal transitions of the formulations. 0.67 g ± 0.06 g of a gelatin mixture was packed into the stainless-steel cell. The reference cell was filled with an equivalent amount of reverse osmosis water. Samples were then analysed using the following profile: initially the sample was cooled to a temperature of 0°C and then held there for 60 minutes. A heating ramp was applied at a scanning rate of 1.2°C/min up to 60°C and then cooled at the same rate back to 0°C, where it was held for another 60 minutes. This cycle was repeated twice, so that 3 heating and 3 cooling curves were obtained in total. The maximum temperature of 60˚C was used as all the transitions were complete within this temperature range (Iijima et al., 2007, Wang et al., 2015). Gelling temperatures were determined as the onset of the exothermic peak.

2.3.2. Rheological measurements

Rheological measurements were performed on a Kinexus pro rheometer (Malvern, UK). Three different tests were undertaken: (1) single frequency, (2) frequency sweeps and (3) a custom-made profile to mimic the extrusion process.

Oscillation test at a single frequency

An oscillation test undertaken at a single frequency was conducted at a frequency of 1 Hz and a strain of 1%. The sample was loaded at 60˚C and cooled at a rate of 1˚C/min to 20˚C, during which the evolution of the G' and loss modulus (G") were recorded. A serrated 60mm parallel plate geometry was used, with a gap of 1mm for the formulations with κC, and a gap of 0.35 mm for the formulation without κC. This geometry was used in order to avoid slip and a small amount of silicon oil was spread around the lip of the geometry, to act as an oil trap in order to prevent evaporation of the mixture.

Frequency sweep
Frequency sweeps were obtained for all the samples measuring the G' and G" through a range of applied frequency (0.1-10 Hz). This range was within the linear viscoelastic region of all materials, as determined by amplitude sweeps (data not shown). The tests were undertaken at 20, 30, 40 and 50˚C, apart from the 5% gelatin formulation, which was only tested up to 40˚C, due to the sensitivity of the rheometer. A serrated plate was used with a gap of 0.35mm at temperatures above the gelling temperatures of each of the materials and a gap of 1mm at temperatures tested below the gelling temperatures. The only exception was the 5% gelatin, where a gap of 0.35mm was used for all measurements, due to its low viscosity.

Custom-made profile to mimic the extrusion process
A custom-made extrusion sequence was run in order to simulate how the material would behave as it passed through the nozzle and post-extrusion. When the material passes through the nozzle, it will experience a shearing force and a temperature drop. Both of these variables will affect how the material will flow, therefore it was important to investigate how they affected the material's behaviour. Once the material was extruded, it needed to have a fast recovery rate, in order for it not to spread and also be able to support the weight of any subsequent layers. A two-part sequence was created; the first part investigated how the viscosity of the material was affected through a range of temperatures. The temperature range was reduced from 40˚C-20˚C for the 5% gelatin only and from 50˚C - 20˚C for the gelatin with κC mixtures. A lower temperature range was used for the formulation with just gelatin, as the properties of this mixture at higher temperatures were outside the sensitivity of the rheometer used. The average shear rate within the nozzle was determined using equation 1.

$$\dot{\gamma} = \frac{4Q}{\pi R^3} \quad\quad [1]$$

Where $\dot{\gamma}$ is the shear rate, Q is the flow rate and R is the radius of the nozzle.

Initially, the flow rate was found by printing a shape of known volume (10.26 ml) and recording the time taken to print. The flow rate was then determined using equation 2.

$$Q = \frac{V}{t} \quad\quad [2]$$

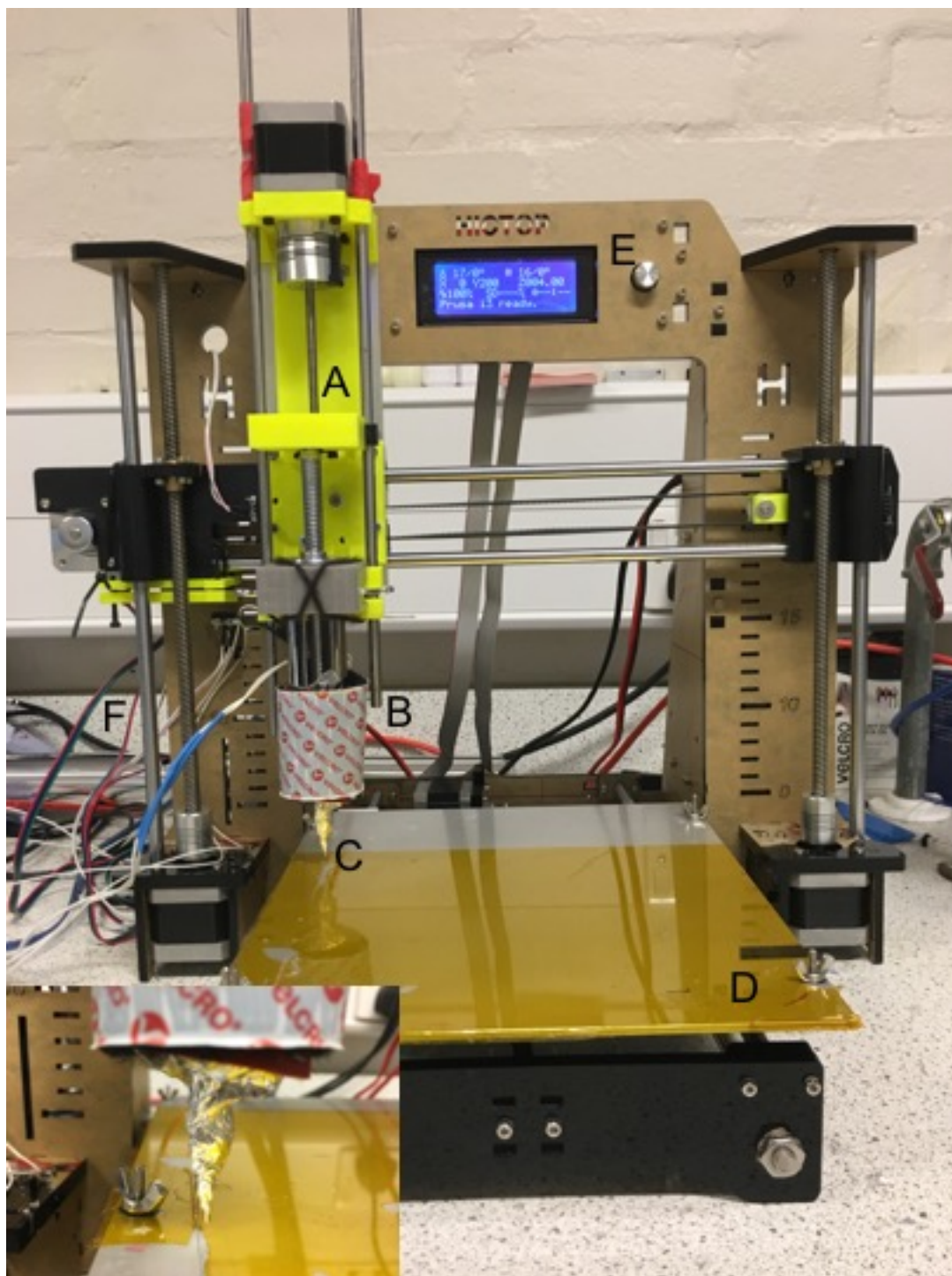201   *Where V is the volume of the printed part and t is the time.*

202

203   The shear rate applied to the material during extrusion through the syringe barrel

204   (needle) was calculated to be of the order of 100 s^{-1}, closely corresponding to previous

205   data presented by Li et al. (2016). The second part of the sequence measured the G'

206   and G" over 10 minutes at a frequency of 1Hz and strain of 0.1%. A serrated plate

207   geometry was used for all these tests, with a gap of 1 mm.

208

209   2.4.   Creation and use of the syringe pump printer

210   The custom-made FDM printer was created by modifying a commercially available

211   Hictop Prusa i3 printer. Firstly, the original nozzle was replaced with a 30 ml metal

212   syringe and a back plate which was designed and printed in plastic. The syringe was

213   encased in a silicone heater pad and controlled using a stepper motor connected to a

214   screw plunger. A metal needle of 0.6 mm diameter, purchased from TECHCON

215   (Hampshire, UK) was used. During the printing process, the syringe was loaded with

216   approximately 15 ml of material (due to the height of the heater pad only covering this

217   much of the syringe) and then the needle was attached and insulated using aluminium

218   foil in order to prevent temperature loss. The syringe was attached to the back plate

219   and held there using printed clasps during the printing process. Figure 1 shows a

220   labelled picture of the syringe printer, with the insert showing a close-up of the

221   insulated needle.

222

223

224

The software used to control the printer was 'Repetier'. In order to create the object, a computer-aided design (CAD) model of the object was inputted into the software (Wong and Hernandez, 2012). The software then 'slices' the object into layers and

232 calculates a path that is then used for the creation of the object. During the printing
233 process, the syringe followed this path and extruded material where necessary, in
234 order to create the shape.

235

236 Before each print the bed level was calibrated manually at the four corners of the bed
237 by using a 100 micron gauge. In all cases, systems were printed at ambient
238 temperatures without the aid of external cooling apparatus. During the prints, the
239 printing speed was set to 10 mm/s and the non-print moving speed was set to 100
240 mm/s. The layer height of the objects was maintained at 0.3 mm for all of the layers.

241

242 ## 2.5. Statistical analysis
243 All of the µDSC and rheological experiments have been repeated in triplicate, while
244 the printed squares have been repeated 6 times. All of the data has been presented
245 as the mean of the results ± 1 standard deviation. Data analysis of the width and the
246 heights of the printed squares was processed with SigmaPlot software, with
247 differences of $p < 0.05$ considered to be significant.

248

249 ## 3. Results and discussion
250 Initially, within this project, mixtures of just gelatin were investigated for the extrusion
251 process, because of their high gel strength (Gómez-Guillén et al., 2011). However,
252 conversion of the coils to helices in gelatin is a slow process (Harrington and Morris,
253 2009), which meant that the printed objects did not retain their shape after printing. κC
254 was added in order to accelerate the gelation of the system enabling better shape
255 retention.

256

257 ## 3.1. Thermal properties of the gelatin and κC mixtures
258 The behaviour of the material within the nozzle will be affected by its thermal
259 properties. such properties of the various printing materials (5% gelatin and 0, 1, 2 and
260 3% κC) were investigated using a µDSC and rheological techniques.

261

262 Figure 2 demonstrates the first cooling cycles, from 60˚C to 0˚C, for 5% gelatin with
263 additions of 0, 1, 2 and 3% κC, found from the µDSC. The 5% gelatin exhibits a single
264 exothermic peak which was attributable to the coil-helix transformation of the gelatin
265 (Michon et al., 1997). The result determined for the 5% gelatin was found to be

266 comparable to the result found by Bohidar and Jena (1993). Following the addition of
267 the various concentrations of the secondary bio-polymer, κC, two exothermic peaks
268 were observed on each of their respective μDSC curves. The broad peak spanning
269 10 to 20 °C was attributed to the gelation of the gelatin. The second peak at much
270 higher temperatures, ca. 30 °C, was attributable to the gelation of the κC as also
271 observed by Wang et al. (2015). The results obtained for the κC were found to be
272 similar to be similar to results obtained by Iijima et al. (2007), who looked at different
273 concentrations of κC.

274
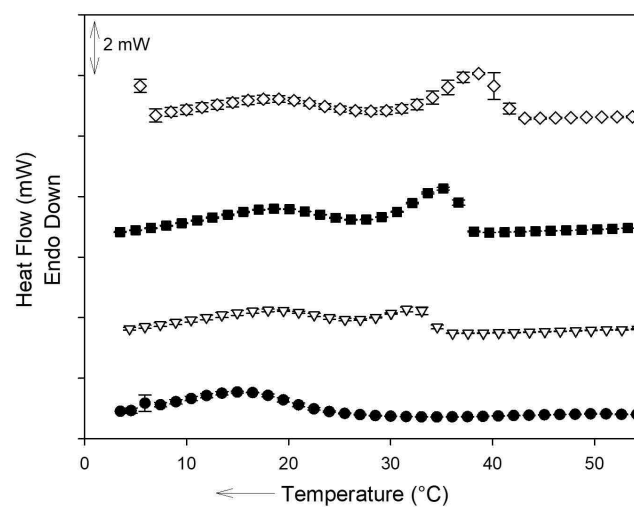
275
276 *Figure 2. μDSC curves of 5% gelatin with 0% KC (●), 1% KC (▽), 2% KC (■), and 3% (◇). (n=3 ± SD).*

277

278 The gelation of the two bio-polymers was further explored using a rotational
279 rheometer. The oscillation test at a single frequency sweep was run from a
280 temperature of 60˚C to 20˚C and the results for the G' and G" for 5% gelatin mixtures
281 with the addition of 0, 1, 2 and 3% κC are shown in Figures 3 A, B, C and D
282 respectively.

283   A

284   B

285   C
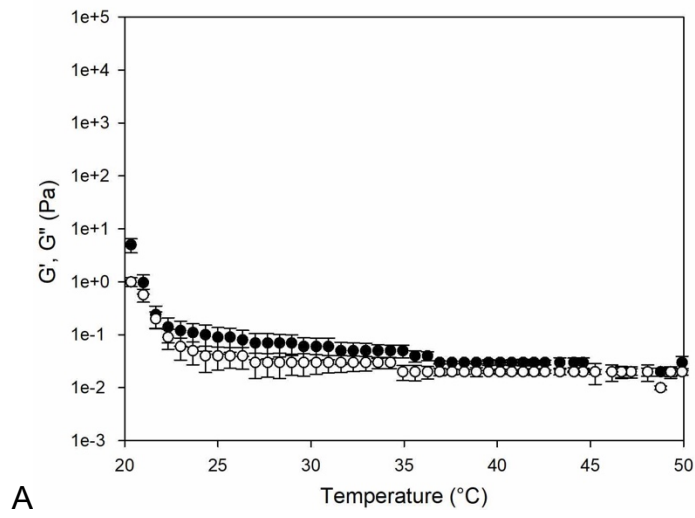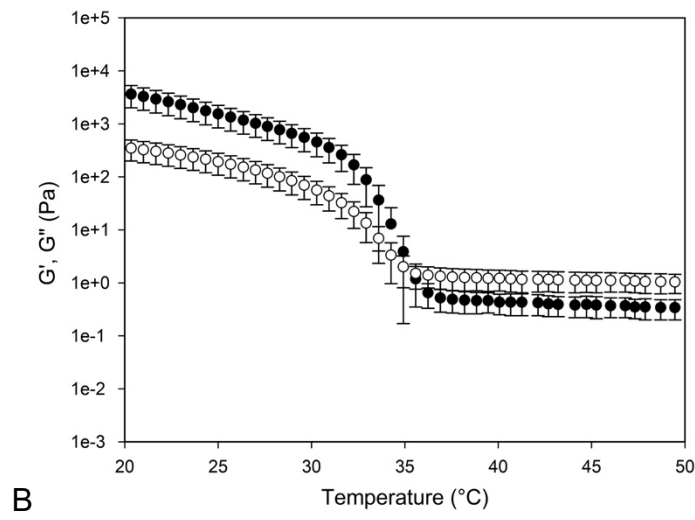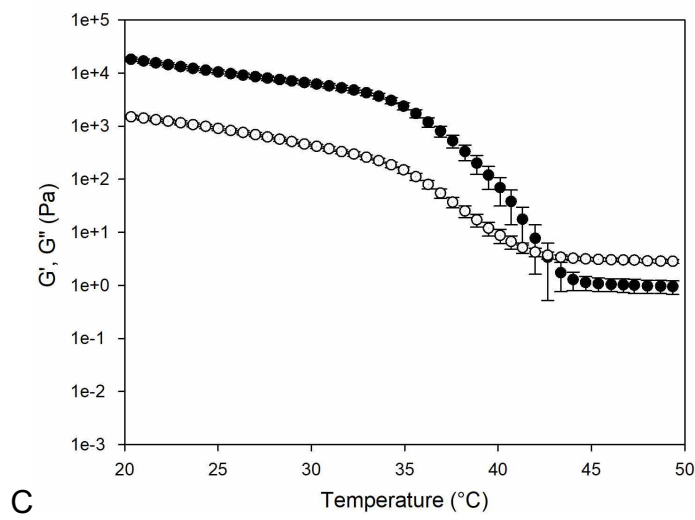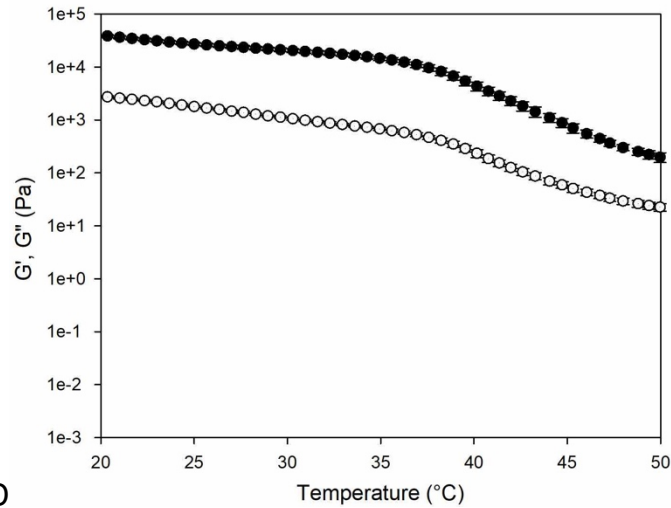
286   D

Figure 3. Figure 3. G' (●) and G" (○) of 5% gelatin and 0% KC (A), 1% KC (B), 2% KC (C) and 3% (D). (n=3 ± SD).

289   G" was greater than G', at high temperatures for all of the formulations, with the
290   exception of 5% gelatin and 3% κC. This result indicated that at high temperatures the
291   systems behaved as a viscoelastic liquid. At 24, 36 and 44 ˚C for the formulations with
292   0, 1 and 2% κC respectively, there was a rapid increase in both G' and G". This
293   increase would appear to be due to the random coils (initially of the κC, and then the
294   gelatin) within the mixture transitioning to ordered helices through hydrogen bonding
295   (Parker and Povey, 2012). A cross-over point occurred between G' and G" shortly after
296   the increase and the temperature this happened was taken as the gelling temperature
297   in accordance with Djabourov et al. (1988). Results obtained for the 5% gelatin
298   solution, using this method, was similar to that obtained by Tosh and Marangoni
299   (2004), who determined the gelling temperature to be 24.5 ˚C. The slightly higher
300   temperature found by Tosh and Marangoni could be attributed to the slower rate and
301   higher frequency that they used.

303   At temperatures lower than the gelling temperature, the G' was greater than the G".
304   This indicated that the mixture behaved as a viscoelastic solid, likely owing to the
305   rheologically significant sample-spanning network of polymeric helices. The
306   formulation with 3% κC displayed a higher G' across the whole range of temperatures
307   tested, indicating that, even at high temperatures, such a high concentration of
308   polymer within the solution resulted in the material being elastically dominated.

310   The results from both the μDSC and the rheological data indicated that the addition of

311   additional κC resulted in a higher temperature being required for gelling (table 1).

312

313   As the temperature was reduced below the gelling point of the κC, gelation of the κC

314   commenced, forming an elastic self-supporting structure which acted as a scaffold for

315   the gelatin. When the temperature was subsequently reduced to the gelling point of

316   the gelatin, gelation of the gelatin commenced leading to further solidification and

317   strengthening of the hydrogel. The control of the printability of the material and the

318   resultant resolution of the product could be enhanced by this two-step mechanism as

319   it would prevent the primary polymer (gelatin) from spreading during the cooling

320   process.

321

322   The gelling temperatures obtained from both the rheometer and the μDSC were found

323   to be very similar. The small difference observed may have been due to the different

324   rates used for each of the pieces of equipment. The results found from the onset of

325   the μDSC were taken forward as the gelling temperature.

326

327   ### 3.2.   Rheological characterisation of the gelatin mixtures

328   It is important to understand the rheological properties of the materials to be printed

329   because the resultant product must not only be edible but it must also be desirable.

330   (Van Vliet, 2013).

331

332   Frequency sweeps were performed on all of the materials at different temperatures,

333   both above and below their gelling temperature. The G' and G" determined from the

334   frequency curves obtained from a mixture of 5% gelatin and 2% κC at 20, 30, 40 and

335   50°C can be seen in Figure 4. The shape of the curves obtained were typical for all of

336   the other formulations.

337

For each of the different materials tested, when the testing temperature was greater than the gelling temperature, both G' and G" were dependent on frequency; this demonstrated that the materials were liquid-like. It was observed that at temperatures greater than the gelling temperatures, the moduli of each formulation exhibited similar values, with a difference of 4, 8, 10 and 3% for 0, 1, 2 and 3% κC, respectively. As a result of the finding that the viscoelastic properties were no longer dependent on the temperature when the gelling point was exceeded, it is likely there would likely be no material benefit to printing at a higher temperature.

When the testing temperature was reduced below the gelling temperatures of each of the four formulations, G' and G" became independent of frequency, indicating confirmation of the solid-like state of the material (Derkach et al., 2015). This result was also observed by del Carmen Núñez-Santiago and Tecante (2007) who investigated the evolution of moduli of 1% κC.

Figure 5 depicts the value of G' and G" for all the four formulations taken from the frequency sweeps, at a value of 1 Hz and at temperatures of 20˚C and 50˚C. At all temperatures tested, as the concentration of κC was increased, the G' increased. This was the result of the synergistic effects of the gelatin and κC (Derkach et al., 2015). The hydrogen bonds formed with κC were stronger than those formed with just gelatin molecules. Costakis et al. (2016) determined that an increase in G' would allow better

363 shape retention post printing. The greater the value of the G' indicated higher gel
364 strength, which would enable the material to retain its shape following extrusion.

365
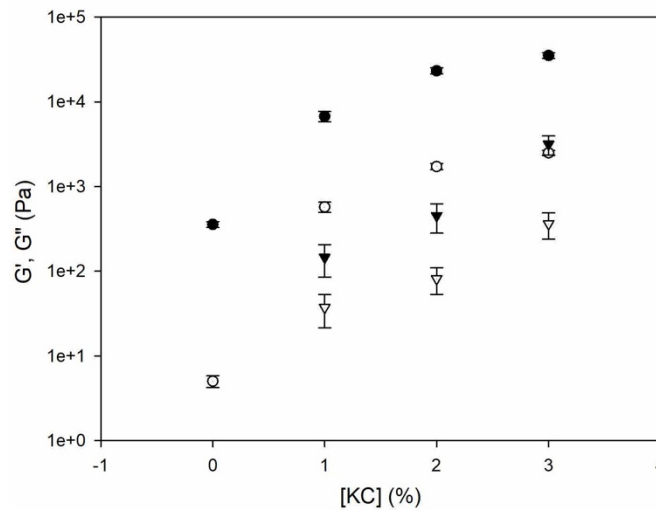
366
367 *Figure 5. Frequency sweeps of 5% gelatin and different concentrations of KC at 20˚C (O) and 50˚C (▽), open symbols are*
368 *the G", while closed symbols are the G'. (n=3 ± SD).*

369

3.3. Creation of an extrusion simulation

371 A simple simulation of the extrusion process was developed using a rotational
372 rheometer in order to determine the behaviour of the material during extrusion. The
373 simulation consisted of two parts: firstly, a viscosity curve was undertaken to mimic
374 the extrusion of the material using the average shear rate established previously;
375 secondly, small deformation rheology was employed to monitor the structuring of the
376 material on the plate post-printing.

377

378 The viscosity curves, at a shear rate of 100 s^{-1}, from a temperature of 60˚C to 20˚C,
379 of all four formulations is shown in Figure 6. There was a rapid increase in viscosity at
380 22˚C, 34˚C, 37˚C and 42˚C for 5% gelatin with 0, 1, 2 and 3% κC respectively. These
381 values were very similar to the gelling temperatures found previously using both the
382 μDSC and the rheometer, this increase in viscosity was therefore attributed to the
383 gelling of the material. The results obtained for the 5% gelatin are in agreement with
384 those obtained by Madhamuthanalli and Bangalore (2014), who determined that at 25
385 ˚C the viscosity was 0.032 Pa.s, while the results for the 1% κC are similar to those
386 obtained by Gabriele et al. (2009).

387

388 It has been noted previously that the minimum material viscosity required to
389 successfully print was 0.03 Pa.s (Murphy and Atala, 2014). Only the formulations with
390 2 and 3% κC were above this minimum viscosity throughout the range of temperatures
391 tested. The viscosities of the formulations with 0 and 1 % κC were below this minimum
392 value of viscosity, until the temperatures exceed their gelling temperatures and the
393 materials started to gel. If these formulations were extruded at a temperature too far
394 above their gelling temperatures, the viscosity might be too low, resulting in material
395 which just flows out of the nozzle, particularly in cases where the surface tension is
396 not sufficiently great to prevent it (He et al., 2015).

397

398 Analysis of the recovery of the material was important in order to determine whether
399 the material would spread after extrusion and whether subsequent layers could be
400 printed onto it. The recovery graphs show how both the G' (figure 7 A) and G" (figure
401 7 B) behaved following removal of the shear whilst at a constant temperature of 20 ˚C.
402 The graph only records results up to 200s as, within this timeframe, any additional
403 layers would be printed. As soon as the shear was removed all of the formulations
404 displayed an elastically dominant system. The time taken for the system to reach an
405 equilibrium, which meant that the system was a solid gel, was a function of κC
406 concentration. The curves were fit to an exponential growth equation, shown in
407 equation 3.

408

409 $$y = y_0 + a(1 - e^{-bt})$$ [3]

410

411 *Where y is G', y_0 is the initial G', a is the final growth, b is the rate of growth and t is*
412 *time.*

413

414 The maximum value of G' found for 3, 2, 1 and 0% κC was found to be 4, 2, 0.6 and
415 0.4 Pa respectively. Once these values had been obtained from each of the individual
416 curves, the recovery of the formulations with 3, 2 and 1% κC at 2 minutes was found
417 to be 75%, 73% and 67% of their maximum G' values respectively. The formulation
418 without the κC only recovered to 45% of its maximum G' value, indicating that the
419 recovery occurred a lot faster for the formulation with κC compared to the formulation
420 without, as a result of the strong interactions between the gelatin and κC molecules.

3.4.   Determination of printability using the rheological data

Printability was evaluated by assessing the uniformity of the extrusion during the printing process along with the accuracy and stability of the printed part (Lille et al., 2017). The temperature control within the printing process was of utmost importance due to the temperature dependence sol-gel transition of gelatin (Billiet et al., 2014). It was found previously that at temperatures higher than the gelling temperature the viscoelastic properties of the material were similar. However, there was a change in the properties when the gelling temperature was reached. In order to determine how much the viscoelastic properties affected the printability, 2D and 3D squares were printed out in each material, at its gelling temperature and at a higher temperature.

Each of the printed squares were intended to measure 20mm x 20mm with a width of 1mm and the extrusion commenced in the bottom left corner. The 2D squares were printed with 1 layer (height of 0.3 mm) and the 3D squares were printed using 4 layers (height of 1.2 mm). By printing both 2D (Figure 8) and 3D (Figure 9) structures of all the formulations, at both their gelling temperatures and a higher temperature, it was possible to determine whether the materials were gelling fast enough to allow layers to be built up.

In order to determine the accuracy of the resultant printed squares, the width and the height of each square was measured. This analysis process was similar to that of Derossi et al. (2017) who measured the heights and width of a fruit-based formulation to determine if their printed snacks matched the design structure. The width of the printed square was measured at the bottom right corner, after the first corner, whilst the height was measured at the four corners and averaged. The level of spreading was determined by the deviation from the intended values.

Table 2 shows the results of the measurement of the width of the 2D and 3D squares printed at both the formulations gelling temperature ($T=T_{gel}$) and at the higher temperature ($T>T_{gel}$) for all systems tested with the addition of κC. Deviation was calculated as the percentage difference between the desired value of 1 mm and the experimental widths found. Neither the 2D nor the 3D squares extruded with 'gelatin only' formulation exhibited a uniform width, therefore these results were not presented.

455   The 2D and 3D squares, obtained by the printing of the formulation with no κC,
456   displayed poor resolution, broken lines and a large amount of spreading. Costakis et
457   al. (2016) determined that materials with a higher G' resulted in better shape retention.
458   The G' for the formulation without any κC was 0.7 kPa resulting in pools of material
459   being formed rather than a solid line. The spreading occurred as the gelation process
460   was not rapid enough to prevent the material from spreading (Wei et al., 2015).

461

462   Spreading of the extruded material also occurred when the formulation with 1% κC
463   was printed. The width of the 2D squares were at least 40% larger than desired at both
464   temperatures printed. The spreading was not only due to the long gelation time of this
465   material and the low G' (ca. 4.5 kPa), but also due to the material phase separating.
466   When subsequent layers were added, more spreading occurred, with a large
467   difference of width observed between the two temperatures used for printing. The
468   squares printed at a higher temperature showed greater levels of spreading (240%)
469   compared to the squares printed at the gelling temperature (150%). The squares
470   printed at a lower temperature reached their gelation temperature faster, which
471   reduced the spreading of the material.

472

473   The width of the 2D squares printed with the addition of 2% κC were observed to be
474   within 10% of the standard value at both temperatures tested. In this instance over
475   73% of the material's structuring was recovered within 200s and that, combined with
476   the high G' (ca. 23 kPa), ensured that spreading was inhibited due to the strong elastic
477   network within the system being created quickly as a result of the fast recovery time.
478   When the 4 layer high, 3D square was printed using the 2% κC formulation, the width
479   of the square spread ca. 70%. This outcome was the result of insufficient adhesion
480   between the subsequent layers, as the material gelled too quickly to bond to the
481   previous layer, resulting in the newly deposited layer sliding off the lower layer. The
482   width of this formulation was similar at both of the temperatures tested for this
483   formulation, again owing to the fast gelation time.

484

485   The width of the 2D square printed with the mixture containing 3% κC was within 10%,
486   when printed at a temperature higher than its gelling temperature. When this
487   formulation was printed at its gelling temperature, the width was found to be a lot wider.

488   In Figure 8D, it can be seen that the square printed at the gelling temperature (42°C)
489   did not produce a shape with solid lines. This was likely to be due to the material
490   gelling within the nozzle itself resulting in extrusion of a solid material. The same
491   broken lines could also be seen when a 3D square was printed at this temperature
492   (Figure 9D). The 2D shape obtained when printing at a higher temperature was within
493   10% of the printed width, due to the fast gelation time and high G' of this material. The
494   4 layer high 3D shapes, printed using the formulation of 3% κC displayed a well printed
495   square, close to the desired width.

496

497   Table 3 documents the heights of the 2D and 3D printed squares at the formulations
498   gelling temperature (T=T_{gel}) and at the higher temperature (T>T_{gel}). The deviation was
499   calculated as the percentage difference between the desired values of 0.3 mm for 1
500   layer and 1.2 mm for 4 layers and the determined experimental heights. For the
501   formulation without κC, both the 2D and 3D squares achieved a greater than desired
502   height at the lower temperature tested. During printing of these squares, it was
503   observed that the material was dragged along, leading to excess material forming
504   pools rather than lines and resulting in the higher than expected heights. It would
505   appear that some structuring was occurring within this system, but not fast enough to
506   prevent the pools from forming. The height of the 2D printed square, printed at the
507   higher temperature (40°C) was lower than was desired due to the material not
508   structuring in time, therefore not able to hold the shape together. The height of the 3D
509   printed square at the higher temperature was observed to be over 50% less than the
510   desired height. The higher printing temperature and slow elastic network formation led
511   to the gelatin acting like a viscoelastic liquid. A 3D network of polymers was not able
512   to form, resulting in spreading of the material as the lower structure was unable to
513   support the subsequent layers and therefore the desired height was not achieved.

514

515   The table illustrates that, despite the fact both spread beyond the desired width, there
516   was a height difference between the 1% κC 2D squares printed at the gelling
517   temperature and the higher temperatures. For the formulation with 1% κC, an elastic
518   network began to form at 35°C. Printing at a slightly higher temperature caused a
519   minimal delay in the formation of the network. This delay in time prior to network
520   development increased when the printing temperature was increased to 50°C. The

result of this time differential led to the square printed at the lower temperature achieving a greater height as a result of the quicker formation of the network. Using the same formulation, the printed height the 3D shapes achieved was about 80% less than the desired height. Despite the fact that the width was affected by spreading of the printed material some height was achieved. This indicates that the observed large width discovered was likely due to the phase separation of the material.

For the formulation with 2% κC, the same printed height was achieved for the 2D squares when extruding at both temperatures. The fast gelation time of this material ensured that the temperatures did not affect the mixture. However, at both temperatures, when the 3D squares were printed the height was greater than desired along with the width. This was caused by the lack of bonding between the layers leading to material which did not slip off the lower layers gelling on top of the previous layer, leading to the height of the squares being greater than desired.

The squares obtained from printing the 5% gelatin and 3% κC mixture at its gelling temperature were broken and ill defined. The height of the 2D shapes was similar to the squares printed with the mixture printed with 2% κC. However, the squares themselves were dissimilar with the uneven printing of the former giving a false impression of height. When printed at the higher temperature, the height of the 2D and 3D squares were identical to the heights achieved with the formulation of 5% gelatin and 2% κC. The fast gelation time of this material enabled the printed object to retain the desired shape.

As the concentration of the κC within the system was increased, the printability of the system improved, with printed squares of the formulation of 5% gelatin and 3% κC producing squares closest to the desired shape.

4. Conclusions

This paper presents an assessment of the printability of 5% gelatin solutions with additions of κC in order to establish design rules for the printing of thermally gelling hydrocolloids. It was found that in order to print well defined structures, the magnitude of the G' needed to be greater than 2 kPa at the printing temperature and greater than

554 23 kPa at the temperature of the environment in which the object was being printed
555 (during these experiments the temperature of the room was set to 20°C). It was also
556 necessary for the formulation to recover at least 73% of its maximum G' within 200s
557 which facilitated the rapid formation of an elastic network necessary to prevent
558 spreading and achieve shape retention.

559

560 It was established that the printing temperature affected the printability of the different
561 formulations. The addition of κC resulted in an increase in the gelling temperature
562 which enabled greater control of the printing as compared to the formulation of just
563 gelatin alone, which gelled just above room temperature. The increased gelling
564 temperature provided a greater temperature differential when printing at room
565 temperature, allowing the material to solidify faster and create the desired shape. In
566 general, the objects printed with the different formulations at their gelling temperatures
567 achieved a more defined structure with less spreading of the material. The exception
568 was of the formulation of 5% gelatin and 3% κC printed at room temperature, which
569 displayed poor printed shapes. This was due to the magnitude of the G' being too
570 great at this temperature, ca. 6 kPa which led to structuring within the nozzle, resulting
571 in the formulation being extruded as solid-like and leading to broken lines. When this
572 formulation was printed at an increased temperature, good printability was achieved.

573

574 The influence of rheological and thermal transitions on the printability of
575 thermoreversible materials outlined above could be applied to 3D printing of various
576 other materials undergoing the same thermal gelation process which will be the focus
577 of subsequent studies.

578

582

583 **References**

584 ANTONOV, Y. A. & GONÇALVES, M. 1999. Phase separation in aqueous gelatin–κ-
585   carrageenan systems. *Food Hydrocolloids,* 13**,** 517-524.
586 BILLIET, T., GEVAERT, E., DE SCHRYVER, T., CORNELISSEN, M. & DUBRUEL, P. 2014. The 3D
587   printing of gelatin methacrylamide cell-laden tissue-engineered constructs with high
588   cell viability. *Biomaterials,* 35**,** 49-62.

BOHIDAR, H. B. & JENA, S. S. 1993. Kinetics of sol–gel transition in thermoreversible gelation of gelatin. *The Journal of Chemical Physics,* 98**,** 8970-8977.

COHEN, D. L., LIPTON, J. I., CUTLER, M., COULTER, D., VESCO, A. & LIPSON, H. Hydrocolloid printing: a novel platform for customized food production. Solid Freeform Fabrication Symposium (SFF'09), 2009.

COSTAKIS, W. J., RUESCHHOFF, L. M., DIAZ-CANO, A. I., YOUNGBLOOD, J. P. & TRICE, R. W. 2016. Additive manufacturing of boron carbide via continuous filament direct ink writing of aqueous ceramic suspensions. *Journal of the European Ceramic Society,* 36**,** 3249-3256.

CRUMP, S. S. 1992. Apparatus and method for creating three-dimensional objects. Google Patents.

DEL CARMEN NÚÑEZ-SANTIAGO, M. & TECANTE, A. 2007. Rheological and calorimetric study of the sol–gel transition of κ-carrageenan. *Carbohydrate polymers,* 69**,** 763-773.

DERKACH, S. R., ILYIN, S. O., MAKLAKOVA, A. A., KULICHIKHIN, V. G. & MALKIN, A. Y. 2015. The rheology of gelatin hydrogels modified by κ-carrageenan. *LWT-Food Science and Technology,* 63**,** 612-619.

DEROSSI, A., CAPORIZZI, R., AZZOLLINI, D. & SEVERINI, C. 2017. Application of 3D printing for customized food. A case on the development of a fruit-based snack for children. *Journal of Food Engineering*.

DIAZ, J., V., VAN BOMMEL, K., J,C. , NOORT, M., W-J. & HENKET, J. B., P. 2014. *Method for the production of edible objects using sls and food products*. France patent application WO2014193226A1.

DIAZ, J. V., VAN BOMMEL, K. J. C., NOORT, M. W.-J., HENKET, J. & BRIËR, P. 2016. Method for the production of edible objects using sls and food products. Google Patents.

DJABOUROV, M., LEBLOND, J. & PAPON, P. 1988. Gelation of aqueous gelatin solutions. II. Rheology of the sol-gel transition. *Journal de Physique,* 49**,** 333-343.

GABRIELE, A., SPYROPOULOS, F. & NORTON, I. T. 2009. Kinetic study of fluid gel formation and viscoelastic response with kappa-carrageenan. *Food Hydrocolloids,* 23**,** 2054-2061.

GODOI, F. C., PRAKASH, S. & BHANDARI, B. R. 2016. 3d printing technologies applied for food design: Status and prospects. *Journal of Food Engineering,* 179**,** 44-54.

GÓMEZ-GUILLÉN, M. C., GIMÉNEZ, B., LÓPEZ-CABALLERO, M. E. & MONTERO, M. P. 2011. Functional and bioactive properties of collagen and gelatin from alternative sources: A review. *Food Hydrocolloids,* 25**,** 1813-1827.

HAO, L., MELLOR, S., SEAMAN, O., HENDERSON, J., SEWELL, N. & SLOAN, M. 2010. Material characterisation and process development for chocolate additive layer manufacturing. *Virtual and Physical Prototyping,* 5**,** 57-64.

HARRINGTON, J. C. & MORRIS, E. R. 2009. Conformational ordering and gelation of gelatin in mixtures with soluble polysaccharides. *Food Hydrocolloids,* 23**,** 327-336.

HE, Y., QIU, J., FU, J., ZHANG, J., REN, Y. & LIU, A. 2015. Printing 3D microfluidic chips with a 3D sugar printer. *Microfluidics and Nanofluidics,* 19**,** 447-456.

IIJIMA, M., HATAKEYAMA, T., TAKAHASHI, M. & HATAKEYAMA, H. 2007. Effect of thermal history on kappa-carrageenan hydrogelation by differential scanning calorimetry. *Thermochimica Acta,* 452**,** 53-58.

JOLY-DUHAMEL, C., HELLIO, D., AJDARI, A. & DJABOUROV, M. 2002. All Gelatin Networks: 2. The Master Curve for Elasticity. *Langmuir,* 18**,** 7158-7166.

635   KRUTH, J. P., LEU, M. C. & NAKAGAWA, T. 1998. Progress in Additive Manufacturing and
636   Rapid Prototyping. *CIRP Annals - Manufacturing Technology,* 47**,** 525-540.
637   LI, H., LIU, S. & LIN, L. 2016. Rheological study on 3D printability of alginate hydrogel and
638   effect of graphene oxide. *2016,* 2.
639   LILLE, M., NURMELA, A., NORDLUND, E., METSÄ-KORTELAINEN, S. & SOZER, N. 2017.
640   Applicability of protein and fiber-rich food materials in extrusion-based 3D printing.
641   *Journal of Food Engineering.*
642   LIU, Z., ZHANG, M., BHANDARI, B. & YANG, C. 2017. Impact of rheological properties of
643   mashed potatoes on 3D printing. *Journal of Food Engineering.*
644   MADHAMUTHANALLI, C. V. & BANGALORE, S. A. 2014. Rheological and physico-chemical
645   properties of gelatin extracted from the skin of a few species of freshwater carp.
646   *International journal of food science & technology,* 49**,** 1758-1764.
647   MANGIONE, M. R., GIACOMAZZA, D., BULONE, D., MARTORANA, V., CAVALLARO, G. & SAN
648   BIAGIO, P. L. 2005. K+ and Na+ effects on the gelation properties of κ-Carrageenan.
649   *Biophysical Chemistry,* 113**,** 129-135.
650   MICHON, C., CUVELIER, G., RELKIN, P. & LAUNAY, B. 1997. Influence of thermal history on
651   the stability of gelatin gels. *International Journal of Biological Macromolecules,* 20**,**
652   259-264.
653   MORRISON, N. A., CLARK, R. C., CHEN, Y. L., TALASHEK, T. & SWORN, G. 1999. Gelatin
654   alternatives for the food industry. *In:* NISHINARI, K. *Physical Chemistry and Industrial*
655   *Application of Gellan Gum.* Berlin, Heidelberg: Springer Berlin Heidelberg.
656   MURPHY, S. V. & ATALA, A. 2014. 3D bioprinting of tissues and organs. *Nature*
657   *biotechnology,* 32**,** 773-785.
658   PARKER, N. & POVEY, M. 2012. Ultrasonic study of the gelation of gelatin: phase diagram,
659   hysteresis and kinetics. *Food Hydrocolloids,* 26**,** 99-107.
660   REES, D. A. 1972. Polysaccharide gels. A molecular view *Chem. Ind.***,** 630.
661   TAKAYANAGI, S., OHNO, T., OKAWA, Y., SHIBA, F., KOBAYASHI, H. & KAWAMURA, F. 2000.
662   Sol-gel transition of a mixture of gelatin and κ-carrageenan. *The Imaging Science*
663   *Journal,* 48**,** 193-198.
664   TOSH, S. M. & MARANGONI, A. G. 2004. Determination of the maximum gelation
665   temperature in gelatin gels. *Applied Physics Letters,* 84**,** 4242-4244.
666   VAN VLIET, T. 2013. *Rheology and fracture mechanics of foods*, CRC Press.
667   WANG, L., CAO, Y., ZHANG, K., FANG, Y., NISHINARI, K. & PHILLIPS, G. O. 2015. Hydrogen
668   bonding enhances the electrostatic complex coacervation between κ-carrageenan
669   and gelatin. *Colloids and Surfaces A: Physicochemical and Engineering Aspects,* 482**,**
670   604-610.
671   WEI, J., WANG, J., SU, S., WANG, S., QIU, J., ZHANG, Z., CHRISTOPHER, G., NING, F. & CONG,
672   W. 2015. 3D printing of an extremely tough hydrogel. *Rsc Advances,* 5**,** 81324-81329.
673   WOHLERS, T. & GORNET, T. 2012. History of additive manufacturing.
674   WONG, K. V. & HERNANDEZ, A. 2012. A Review of Additive Manufacturing. *ISRN Mechanical*
675   *Engineering,* 2012**,** 10.
676   YANG, F., ZHANG, M., BHANDARI, B. & LIU, Y. 2018. Investigation on lemon juice gel as food
677   material for 3D printing and optimization of printing parameters. *LWT-Food Science*
678   *and Technology,* 87**,** 67-76.
679
680

681 Table 1

	Gelling temperature (˚C)	
	Onset of exotherm	**Cross-over temperature**
5% gelatin	24 ± 0.4	22 ± 0.2
5% gelatin and 1% κC	36 ± 0.4	36 ± 1.3
5% gelatin and 2% κC	39 ± 0.01	42 ± 0.9
5% gelatin and 3% κC	42 ± 0.01	-

682

683

684   Table 2

		Concentration of κC added (%)					
		1		**2**		**3**	
	No. of layers	**Width (mm)**	**Deviation (%)**	**Width (mm)**	**Deviation (%)**	**Width (mm)**	**Deviation (%)**
T=T$_{Gel}$	**1**	1.6 ± 0.1^a	60	1.1 ± 0.1^{ab}	10	1.6 ± 0.5^b	60
	4	2.5 ± 0.4^a	150	1.8 ± 0.2	80	1.7 ± 0.7^a	70
T>>T$_{Gel}$	**1**	1.4 ± 0.2^{ab}	40	1.1 ± 0.05^a	10	1.1 ± 0.1^b	10
	4	3.4 ± 0.6^{ab}	240	1.7 ± 0.2^a	70	1.4 ± 0.2^b	40

685
686

687   Table 3

	No. of Layers	Concentration of κC added (%)							
		0		**1**		**2**		**3**	
		Height (mm)	Deviation (%)	Height (mm)	Deviation (%)	Height (mm)	Deviation (%)	Height (mm)	Deviation (%)
$T=T_{Gel}$	**1**	0.5 ± 0.08^{abc}	67	0.3 ± 0.09^{ad}	0	0.2 ± 0.08^{b}	- 33	0.2 ± 0.06^{cd}	- 33
	4	1.6 ± 0.1^{abc}	33	1.0 ± 0.2^{ad}	- 17	1.3 ± 0.2^{bde}	8	0.9 ± 0.05^{ce}	- 25
$T \gg T_{Gel}$	**1**	0.2 ± 0.1	- 33	0.2 ± 0.07	- 33	0.2 ± 0.07	- 33	0.2 ± 0.04	- 33
	4	$0.5 \pm 0.1_{abc}$	- 58	0.9 ± 0.2^{ade}	- 25	1.4 ± 0.1^{bdf}	17	1.3 ± 0.1^{cef}	8

688